

## Diffusion Controlled Corrosion in Gas Sparged Systems

S. A. Nosier, M. I. El-Khiary, M. A. Nasr, and A. A. Mubarak

Department of Chemical Engineering, Faculty of Engineering,  
Alexandria University, Alexandria, Egypt

Original scientific paper

Received: June 6, 2005

Accepted: December 10, 2005

The rate of diffusion – controlled corrosion of the walls of rectangular bubble column and a liquid has been studied with the copper dissolution technique. Variables studied were superficial air velocity, initial height of solution in the column, physical properties of the solution, and the presence of suspended solids with different concentrations and different particle diameter. The rate of diffusion – controlled corrosion in solution free solids was given by the equation

$$J = 0.232 (Fr \cdot Re)^{-0.22} (L/d_e)^{-0.169}$$

while for the presence of suspended solids, the data were correlated by the equation

$$J = 0.171 (Fr \cdot Re)^{-0.214} (L/d_p)^{0.187}$$

The presence of suspended solids increases the rate of diffusion – controlled corrosion by an amount ranging from 5 to 16 %.

*Key words:*

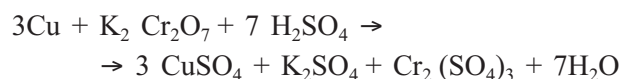
Bubble columns, mass transfer, diffusion – controlled corrosion, suspended solids

### Introduction

Bubble column reactors are now being extensively used in a wide variety of chemical and biochemical processes. Particularly in hydrogenation, oxidation, fermentation, petroleum refining, coal liquefaction, wastewater treatment<sup>1–3</sup> etc, where the overall production rate is often controlled by the gas-liquid interfacial mass transfer, the bubble column reactors are very effective. Bubble column reactors are the type of reactors, which not only provide a significant interfacial mass transfer area, but are also very simple in design and no mechanical agitator is required. Various types of these columns and their modifications may be operated in either semi batch or continuous mode. Bubble columns usually handle corrosive fluids and suffer severely from corrosion. The rate of corrosion may be determined by the diffusion rate of dissolved oxygen to the corroding surface or by the diffusion rate of corrosion products away from the corroding surface. In view of the enormous financial losses, caused to chemical and food industries due to the corrosion, much attention has been directed to diagnosing and remedying this problem. Therefore, numerous authors have studied the problem of corrosion in pipe lines,<sup>4</sup> and mechanically agitated vessel.<sup>5–7</sup> In the area of corrosion in bubble columns, most attention has been directed to the corrosion in cylindrical bubble columns,<sup>8</sup> and little attention has been given to other column geometries.

For the experimental verification of the simulation, the copper dissolution method, according to

Gregory and Riddiford,<sup>9</sup> was chosen. It involves contacting a copper surface with a solution of sulphuric acid and potassium dichromate. The dichromate anions acts as an oxidation agent and oxidizes the copper according to the following overall equation:



where chromium is reduced from  $\text{Cr}^{+6}$  to  $\text{Cr}^{+3}$ . Gregory and Riddiford showed the reaction rate to be determined solely by the rate of mass transfer to the wall. Thus the log-mean mass transfer coefficient can be computed directly from the decline in  $\text{Cr}^{+6}$  concentrations. This method was chosen because of the numerous references in the literature to its reliability and ease of use.<sup>10–13</sup>

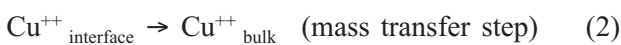
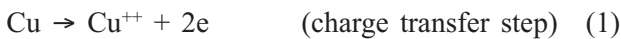
The object of the present work is to study the rate of diffusion-controlled corrosion in rectangular bubble column. Further more, the presence of suspended solids in the bubble column enhance the rate of corrosion, so, the present study was also addressed to cover this point. The present finding was conducted by measuring the rate of diffusion-controlled dissolution of copper walls of the rectangular bubble column in acidified chromate solution.

The present work aims also to compare between the present data and the previous data obtained for diffusion controlled mass transfer in cylindrical bubble columns.

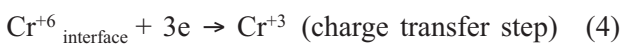
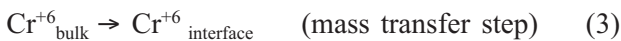
## Theory

According to the theory of corrosion, the overall corrosion reaction consists of two parallel simultaneous reactions, a cathodic reaction and anodic reaction, each of these reactions is a heterogeneous reaction which involves two steps, a charge transfer step and a mass transfer step. In the acidic medium ( $\text{pH} < 4$ ), the following reactions take place:

### At the anodic sites:

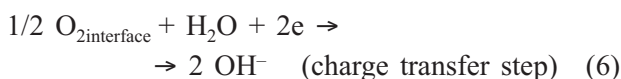
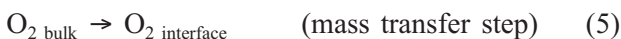


### At the cathodic sites:



The overall rate of corrosion is determined by the slowest step of the above four steps. If the slow step is charge transfer step (reactions 1 and reaction 4), the overall reaction rate is said to be chemically controlled. On the other hand if the slow step is a mass transfer step (reaction 2 and reaction 3), the overall corrosion reaction is said to be diffusion controlled.

In neutral or alkaline medium ( $4 < \text{pH} < 10$ ), the following reactions takes place at the cathodic sites,



In this case, if the rate of transfer of  $\text{O}_2$  from the bulk of solution to the copper surface is slow, the corrosion reaction is said to be diffusion controlled. When corrosion is mass transfer controlled, its rate becomes sensitive to the prevailing hydrodynamic conditions, namely, the flow rate of solution, viscosity and density.

Side reactions between the cathodic product and the anodic product may lead to the formation of porous solid film of corrosion product, e.g. an oxide on the corroding metal surface. Kinetics studies of industrial corrosion, where dissolved oxygen acts as a depolarizer, have revealed that cathodic reduction of oxygen involves three steps, namely:

i. Mass transfer of dissolved oxygen from the solution bulk to the surface of the porous film, the rate of this step is represented by:

$$N_1 = k_{d1} (c_s - c_1) \quad (7)$$

where  $c_s$  is the saturation solubility of oxygen in the solution bulk;  $c_1$  is oxygen concentration at the solid film.

ii. Diffusion of dissolved oxygen through the porous film to the metal surface, the rate of this step is represented by:

$$N_2 = k_{d2} (c_1 - c_2) \quad (8)$$

where  $c_2$  is oxygen concentration at the metal surface

iii. Reduction of oxygen at the metal surface, the rate of this step is expressed by:

$$N_3 = k_{d3} c_2 \quad (9)$$

where  $k_d$  is the specific reaction rate of  $\text{O}_2$  reduction.

Eliminating  $c_1$  and  $c_2$  from the above equations, dissolved oxygen flux ( $N$ ) under steady state conditions can be expressed by the equation:

$$K = \frac{c_s}{\frac{1}{k_{d1}} + \frac{1}{k_{d2}} + \frac{1}{k_{d3}}} \quad (10)$$

Under conditions which may destroy the film, e.g. high shear stress or the presence of suspended solid particles, the resistance of the film to the rate of oxygen diffusion ( $1/k_{d2}$ ) can be neglected and the rate of corrosion may be:

(i) diffusion controlled if the chemical step of oxygen reduction is much faster than the liquid phase mass transfer step;

(ii) partially controlled;

(iii) chemically controlled if the liquid phase mass transfer step is much faster than the chemical step.

## Experimental technique

The experimental setup is shown in Fig. 1. It consisted of air compressor and plexiglass rectangular column. The inside wall of the column was lined with a rectangular copper sheet of dimensions (8\*8\*80 cm). The back surface of the copper sheet, facing the rectangular column wall, was well insulated with epoxy resin and the front surface facing the solution was the working part. The column was fitted at its bottom with a sintered glass distributor of 11.5 cm. diameter and 0.5 cm thickness. The average pore size of the sintered glass was ranged from 5 to 10  $\mu\text{m}$ . Before each run, the system was first cleaned and a known volume of acidified

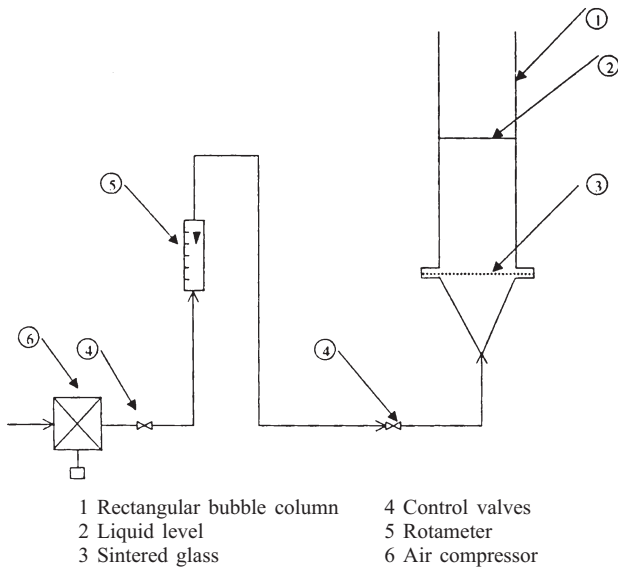


Fig. 1 – Schematic diagram of the experimental setup

chromate solution was introduced into the column. In the mean time, air from the compressor was allowed to pass through the solution at a specified flow rate. The air flow rate was measured by a calibrated rotameter. Two sets of experiments were carried out, the first set was in the absence of suspended solids in which the temperature was ranged from 21 to 29 °C, the superficial air velocities were ranged from 0.3179 to 1.3566 cm s<sup>-1</sup>, the initial solution heights were ranged from 25 to 69 cm and three different solution compositions were used, namely, 3.0 mmol dm<sup>-3</sup> K<sub>2</sub>Cr<sub>2</sub>O<sub>7</sub> + c<sub>x</sub> H<sub>2</sub>SO<sub>4</sub>, c<sub>x</sub> was 0.5, 1, 1.5 mol dm<sup>-3</sup>, respectively.

The second set of the experiments were carried out in the presence of ceramic suspended solids in which the temperature was fixed at 29 °C, the range of the superficial air velocities was as in the first set of the experiments, the initial solution height was fixed at 36 cm, the solution composition was 3.0 mmol dm<sup>-3</sup> K<sub>2</sub>Cr<sub>2</sub>O<sub>7</sub> + 0.5 mol dm<sup>-3</sup> H<sub>2</sub>SO<sub>4</sub>, solid particles diameter was ranged from 0.558 to 1.5 mm, and three mole fraction of solid suspended were used namely, w = 0.05, 0.07 and 0.09 %, respectively. A sample of 2 cm<sup>3</sup> was drawn every 5 min for analysis. Dichromate concentration in the sample was determined by titration against standard ferrous ammonium sulfate using diphenylamine as indicator.<sup>14</sup> Solution density and viscosity, needed for data correlation were determined using a density bottle and Ostwald viscometer, respectively,<sup>15</sup> the diffusivity of dichromate was taken from the literature,<sup>9</sup> and was corrected for the change in temperature and solution viscosity by using the Stokes – Einstein equation:

$$D\mu/T = \text{constant}$$

## Results and discussion

The mass transfer coefficient of the diffusion controlled corrosion of the walls of rectangular bubble columns in acidified chromate solution was obtained under different conditions from the chromate concentration – time data. Fig. 2 shows that the data fit the equation:

$$-V(dc/dt) = K \cdot A \cdot c \quad (11)$$

which on integration yields:

$$\ln(c_0/c) = (K \cdot A \cdot t)/V \quad (12)$$

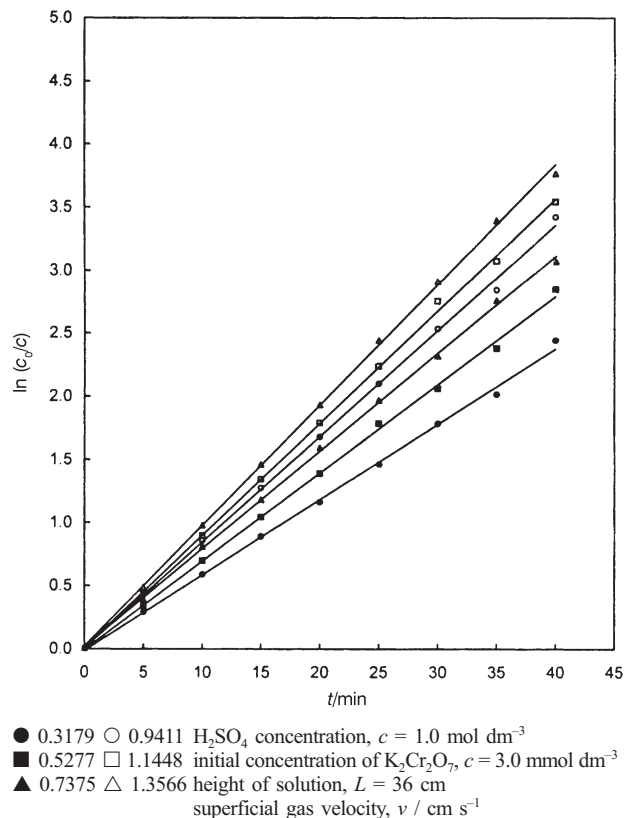


Fig. 2 – Typical  $\ln(c_0/c)$  versus  $t$  plot at different gas superficial velocities

When sampling is used, it is necessary to correct for the resulting volume decrease. The corrected form of the volume equation is

$$V = V_0/V_n \quad (13)$$

where  $V_0$  is the initial volume of solution,  $V_n$  is the volume correction, defined by *Power* and *Ritchie*.<sup>16</sup>

The mass transfer coefficient ( $k_d$ ) was calculated from the slope of the straight line obtained by plotting  $\ln(c_0/c)$  vs. time. Mass transfer coefficient was determined for the five initial solution heights with and without suspended solids under different gas flow rates, different acid concentration, and different percentages of suspended solids.

Fig. 3 shows that the rate of diffusion controlled corrosion increases with increasing superficial air velocity at different ( $Sc$ ) numbers. The data fit the equation:

$$K = a_1 v^{0.321} \quad (14)$$

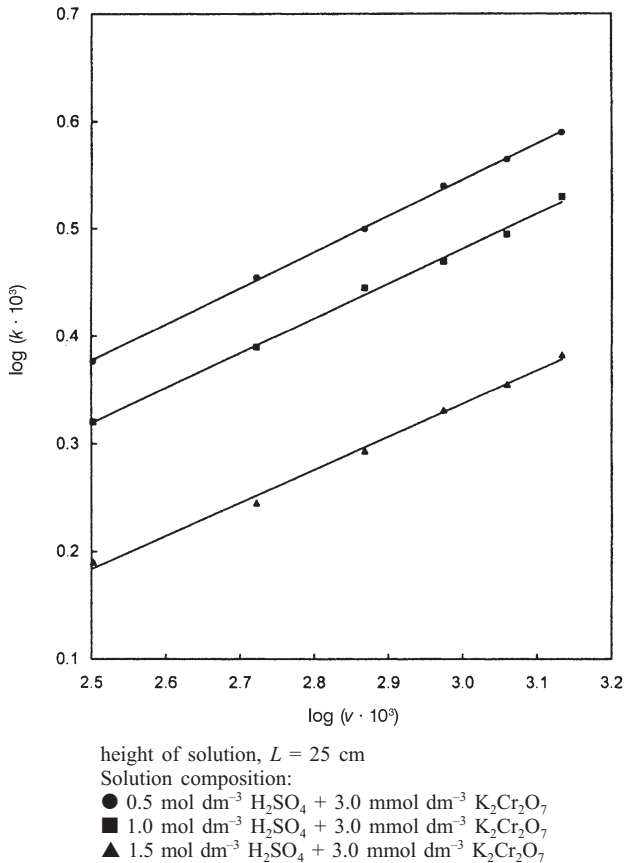


Fig. 3 – Effect of superficial gas velocity on the diffusion-controlled corrosion rate at different acid concentrations

The increase in ( $K$ ) with increasing ( $v$ ) may be attributed to, (i) the rising bubbles collide with the column walls and disturb the diffusion layer with a subsequent increase in the rate of diffusion controlled corrosion; (ii) bubble coalescence or break down in the vicinity of the column wall generates turbulence which penetrates the diffusion layer; (iii) the swarm of the rising bubbles impart radial momentum to the surrounding fluid.<sup>17</sup> The exponent 0.321 is consistent with the range of values obtained by different authors<sup>18–22,11</sup> who studied rates of mass and heat transfer in bubble columns. This agreement confirms that the rate of corrosion of copper metallic rectangular column by dichromate solution under the present conditions is a diffusion-controlled reaction. The decrease in ( $K$ ) with increasing Schmidt number (Fig. 3) may be attributed to the fact that, as  $\text{H}_2\text{SO}_4$  concentration increases, the diffusivity of the dichromate ( $D$ ) de-

creases owing to the increase in solution viscosity and thus increases the diffusion layer thickness.

Fig. 4 shows the effect of the initial solution height on the rate diffusion controlled corrosion at different superficial air velocities. The data fit the equation:

$$K = a_2 L^{-0.171} \quad (15)$$

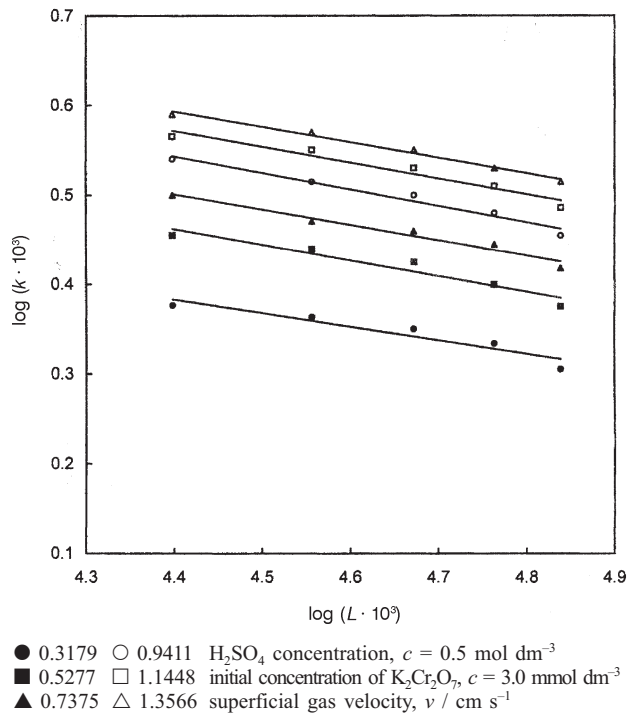


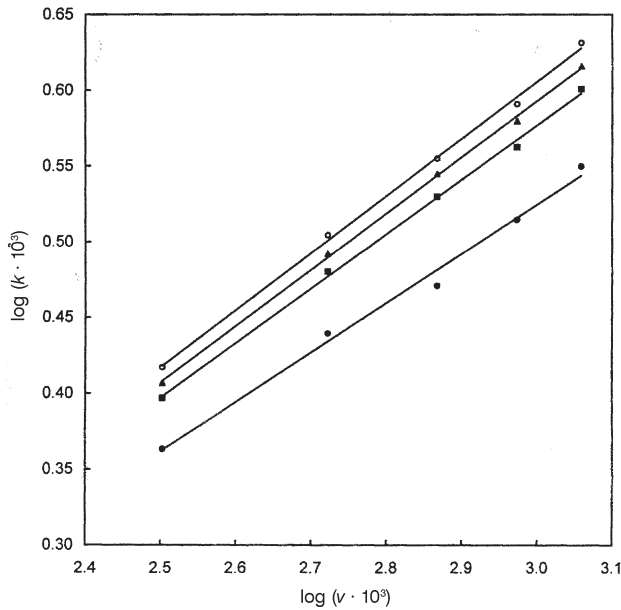
Fig. 4 – Effect of initial solution height on the diffusion-controlled corrosion rate at different superficial gas velocities

The decrease in ( $K$ ) with increasing the initial solution height may be ascribed to the fact, that the flow of liquid/gas dispersion at small liquid height is developing flow; when the flow becomes fully developed, the rate of diffusion – controlled corrosion becomes independent of the liquid height. This phenomena was supported by the previous studies.<sup>11,18–23</sup>

Fig. 5 shows the effect of superficial air velocities on the rate of diffusion controlled corrosion at different solid concentrations. The data fit the equation:

$$K = a_3 v^n \quad (16)$$

The exponent ( $n$ ) ranged from 0.340 to 0.377 depending on concentration and particle size in solution. The presence of suspended solids increases the rate of corrosion by an amount ranging from 5 to 16 %. This increasing in ( $k_d$ ) may be due to (i) the disruption of the diffusion layer at the wall of

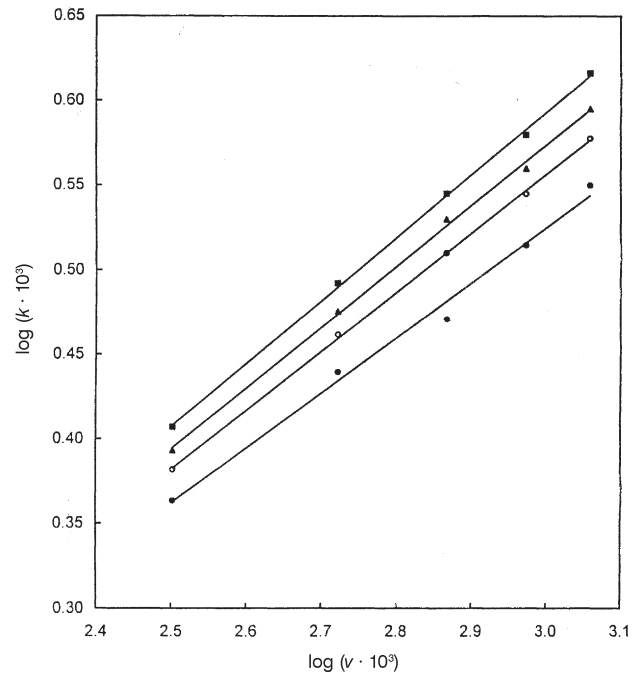


● 0.00 % ▲ 0.07 %  $\text{H}_2\text{SO}_4$  concentration,  $c = 0.5 \text{ mol dm}^{-3}$   
 ■ 0.05 % ○ 0.09 % initial concentration of  $\text{K}_2\text{Cr}_2\text{O}_7$ ,  $c = 3.0 \text{ mmol dm}^{-3}$   
 height of solution,  $L = 36 \text{ cm}$   
 particle diameter of solids =  $0.558 \text{ mm}$   
 $c/p = 0.558 \text{ mm}$   
 fraction of suspended solids:

Fig. 5 – Effect of superficial gas velocity on the diffusion-controlled corrosion rate at different suspended solids concentrations

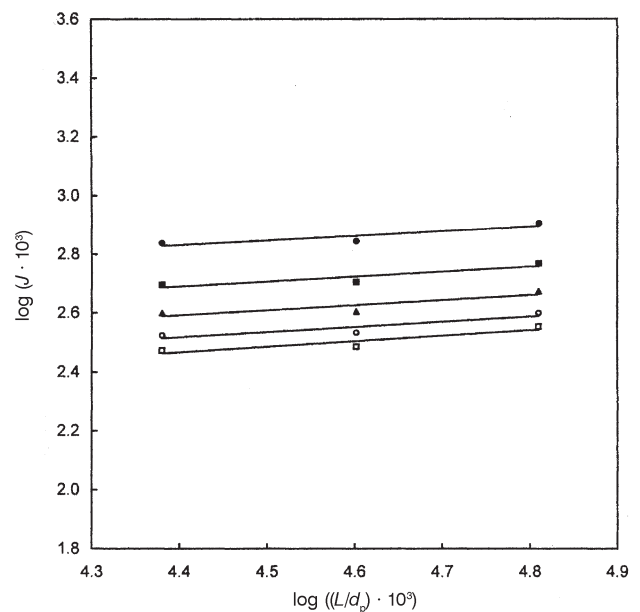
bubble column, by the penetration of the solid particles, generates micro convection, i.e., small scale eddies, the intensity of which depends on the number of particles and the kinetic energy of each particle. This turbulence penetrates the laminar sub-layer of hydrodynamic boundary layer and the diffusion layer with a consequent increase in the rate of corrosion; (ii) when particles impact with the wall, they bring with them a fresh supply of bulk solution and drag away the reacted solution; (iii) the mechanical effect of particles on copper lining surface. These results were supported by the previous studies.<sup>8,24,25</sup> Also, it was found that as the particle size increases, the rate of corrosion decreases (cf. Fig. 6), this phenomena may be explained by the obstruction effect of the larger particle,<sup>26</sup> which hinder the diffusion of the reacting species to the column wall, i.e., the presence of large particles decreases the effective diffusivity of the reacting species with a consequent reduction in the rate of diffusion controlled corrosion.

Two empirical correlations were investigated using the dimensionless groups  $J$ ,  $Fr$ , and  $Re$ , that are usually used in correlating mass and heat transfer in gas stirred vessels. For particle free solution, the initial solution height in the column significantly affects the rate of diffusion controlled corrosion (cf. Fig. 8), an extra dimensionless term was used to account for this effect. This is the ratio be-



● No solids ▲ 0.900  $\text{H}_2\text{SO}_4$  concentration,  $c = 0.5 \text{ mol dm}^{-3}$   
 ■ 0.558 ○ 1.500 initial concentration of  $\text{K}_2\text{Cr}_2\text{O}_7$ ,  
 $c = 3.0 \text{ mmol dm}^{-3}$   
 height of solution,  $L = 36 \text{ cm}$   
 solid to liquid ratio,  $\chi = 7.0$   
 solid particle diameter, mm:

Fig. 6 – Effect of superficial gas velocity on the diffusion-controlled corrosion rate at different particle diameter



□ 0.3179 ■ 0.9411  $\text{H}_2\text{SO}_4$  concentration,  $c = 0.5 \text{ mol dm}^{-3}$   
 ○ 0.5277 ● 1.1448 initial concentration of  $\text{K}_2\text{Cr}_2\text{O}_7$ ,  $c = 3.0 \text{ mmol dm}^{-3}$   
 ▲ 0.7375  
 height of solution,  $L = 36 \text{ cm}$   
 fraction of suspended solids,  $\chi = 5.0$   
 superficial gas velocity,  $v/\text{cm s}^{-1}$

Fig. 7 – Relation between  $J$  and  $(L/d_p)$  at different superficial gas velocities



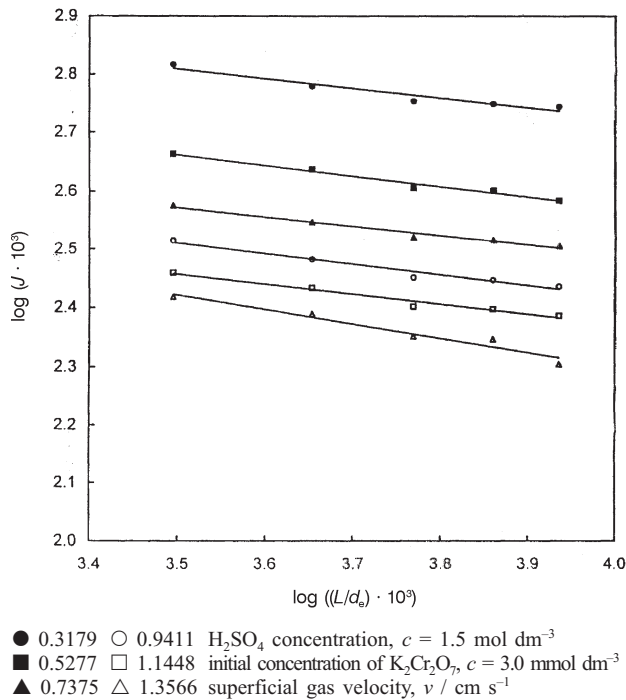


Fig. 8 – Relation between  $J$  and  $(L/d_e)$  at different superficial gas velocities

tween the initial solution height in the column ( $L$ ) and the equivalent diameter of the column ( $d_e$ ). In the presence of particles in the solution, both, the initial height of the solution and the particle size significantly affects the rate of corrosion (Fig. 7), an extra dimensionless term ( $L/d_p$ ) was used to account for this effect. Rectangular bubble column equivalent diameter ( $d_e$ ) was used as the characteristic length in calculating ( $Re$ ).

Fig. 9 shows that for particle free solution under the conditions

$$882 < Sc < 1370, 0.003 < Fr \cdot Re < 0.278$$

$$\text{and } 3.125 < L/d_e >, 8.625$$

The data fit the equation:

$$J = 0.232 (Fr \cdot Re)^{-0.22} (L/d_e)^{-0.169} \quad (17)$$

with an average deviation of  $\pm 3.638 \%$

Fig. 10 shows that in the presence of solid particles under the conditions

$$882 < Sc < 1041, 0.003 < Fr \cdot Re < 0.167$$

$$\text{and } 4.380 < L/d_p < 4.81$$

The data fit the equation:

$$J = 0.171 (Fr \cdot Re)^{-0.214} (L/d_p)^{-0.187} \quad (18)$$

with an average deviation of  $\pm 7.5 \%$

Since there is no significant effect of the characteristics of the gas sparger<sup>19</sup> only one sparger was used in the present study.

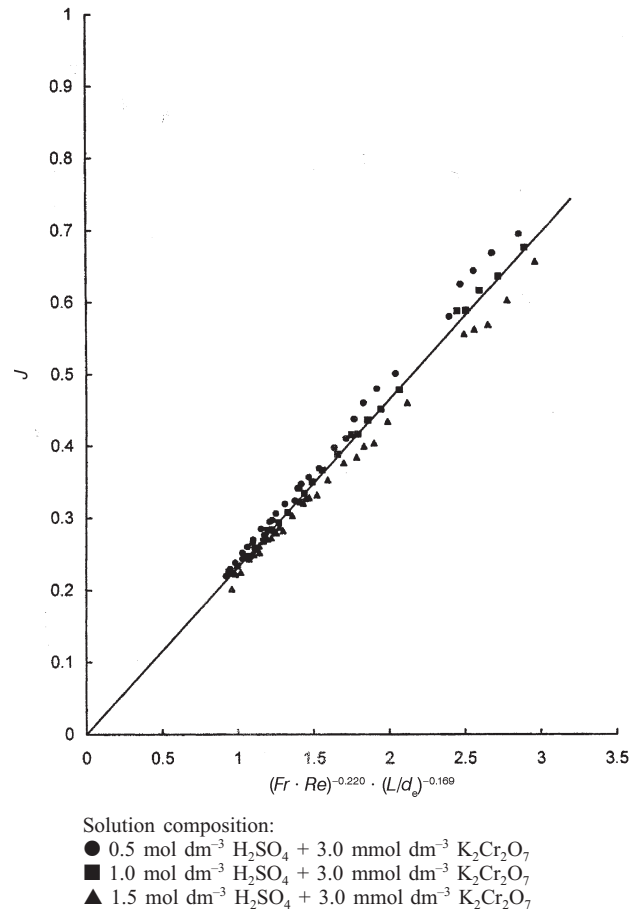


Fig. 9 – Overall mass transfer correlation for solids free solution

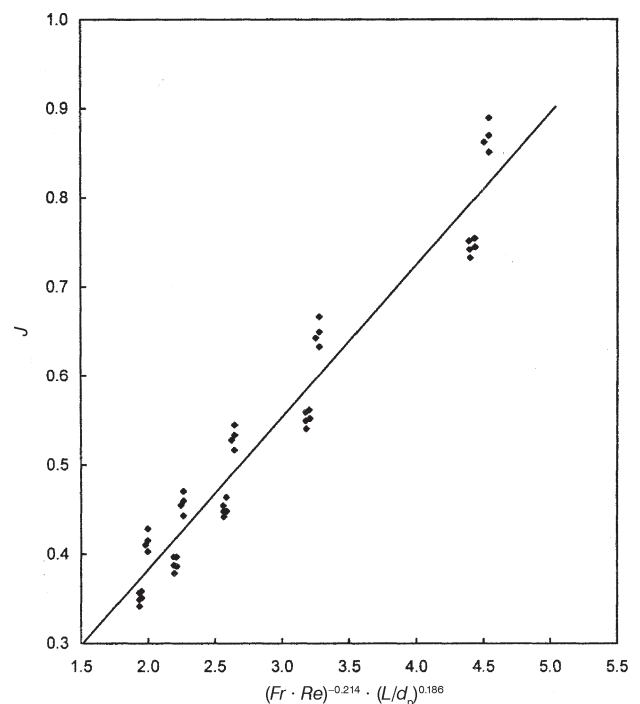


Fig. 10 – Overall mass transfer correlation in the presence of suspended solids in the solution

By comparing between the present data and the data obtained by Bohm et al.,<sup>18</sup> who studied the effect of gas sparging on the rate of mass transfer inside vertical tube using the electrochemical technique, it was found that the rate of mass transfer in the present study under the same conditions was higher than that of Bohm et al findings. The increase in corrosion rate in the present study may be attributed to the fact that, the sharp corners present in the rectangular bubble column lead to turbulence generation in the vicinity of column walls, which enhances the rate of diffusion-controlled corrosion.

## Conclusions

1. Geometry of the bubble columns plays an important role in determining the rate of diffusion controlled-corrosion. For a given set of conditions, a rectangular bubble column suffers higher corrosion than the cylindrical bubble columns. The dimensionless equations obtained in the present work can be used to predict the corrosion rate and hence the corrosion allowance needed to design the gas sparged reactors.

2. Initial height of solution in the column affects the rate of diffusion-controlled corrosion, the higher the height of the solution in the column the lower the rate of corrosion.

3. The rate of diffusion-controlled corrosion was strongly influenced by the physical properties of the solution, the higher the Schmidt numbers the lower the rate of corrosion.

4. The presence of suspended solids in the solution enhances the rate of diffusion controlled corrosion by an amount ranging from 5 to 16 % depending on superficial air velocity, suspended solid concentration, and particle diameter.

## Nomenclature

- $a_1, a_2, a_3$  – constants  
 $A$  – reaction surface area,  $\text{cm}^2$   
 $c_0$  – initial dichromate concentration,  $\text{mol l}^{-1}$   
 $c$  – dichromate concentration at time  $t$ ,  $\text{mol l}^{-1}$   
 $d_e$  – bubble column equivalent diameter,  $\text{cm}$   
 $d_p$  – particle diameter,  $\text{cm}$   
 $D$  – dichromate diffusivity,  $\text{cm}^2 \text{s}^{-1}$   
 $K$  – mass transfer coefficient,  $\text{cm s}^{-1}$   
 $L$  – initial height of electrolyte,  $\text{cm}$   
 $N$  – molar flux,  $\text{mol dm}^{-3} \text{s}^{-1}$   
 $t$  – reaction time,  $\text{s}$   
 $v$  – superficial air velocity,  $\text{cm s}^{-1}$   
 $V_0$  – initial volume of electrolyte,  $\text{cm}^3$   
 $V$  – volume of electrolyte,  $\text{cm}^3$

## Greek letters

- $\mu$  – electrolyte dynamic viscosity,  $\text{g cm}^{-1} \text{s}^{-1}$   
 $\rho$  – electrolyte density,  $\text{g cm}^{-3}$   
 $\delta$  – diffusion layer thickness,  $\text{cm}$

## Dimensionless groups

- $Fr$  – Froude number,  $v^2/gd_e$   
 $J$  – mass transfer  $J$  factor,  $St Sc^{0.66}$   
 $Re$  – Reynolds number,  $\rho v d_e \mu$   
 $Sc$  – Schmidt number,  $\mu/(\rho D)$   
 $St$  – Stanton number,  $K_d/v$

## References

- Nosier, S. A., *Alex. Eng. J.*, **35** (1996) 39.
- Zarraa, M. A., *Hydrometallurgy*, **28** (1992) 423.
- Nosier, S. A., Sallam, S. A., *Sep. Sci. Tech.* **18** (2000) 93.
- Sedahmed, G. H., Abdel-Naby, B. A., Tantawy, S. G., *J. Brit. Corrosion* **25** (1990) 3.
- Ledakowicz, S., Kokuun, R., Brehm, A., *Chem. Eng. Tech.* **55** (1983) 8.
- Warren, S. Beckmann, R. B., *Ind. Eng. Chem. Proc. Des. Dev.* **3** (1965) 311.
- Herndl, G., Mersmann, A., *Chem. Eng. Tech.* **54** (1982) 3.
- Nosier, S. A., *Materials Letters* **31**(1997) 291.
- Greggory, D. P., Riddiford, A. C., *J. Electrochem. Soc.* **107** (1960) 950
- Hirose, T., Mori, Y., Sato, Y., *J. Chem. Eng. Jpn.* **7**(1) (1974) 19.
- Patil, V. K., Sharma, M. M., *Chem. Eng. Res. Dev.*, **61** (1983) 21.
- Zarraa, M., El-Tawil, Y., Farag, H., El-Abd. M., Sedahmed, G., *Chem. Eng. J* **47** (1991) 187.
- Nishikawa, M., Inui, K., Yonezawa, Y., Nagata, S., *Int. Chem Eng.* **16** 40 (1976) 714.
- Vogel, A. I., *A text book of quantitative inorganic analysis 3<sup>rd</sup> Edition* (Longmans, London 1961).
- Findley, A., Kitchener, J. K., *Practical physical chemistry* (Longmans, London 1965).
- Power, G. P., Ritchie, I. M., In: Conway, B.E Bockris, J. O. M.(Eds), *Modern aspect of electrochemistry*, **11** (1975) 199.
- Kast, W., *Chem. Ing. Tech.* **35** (1963) 785.
- Cavatorta, O. N., Bohm, U., *Chem. Eng. Res. Dev.*, **66** (1988) 265.
- Ibl, N., Kind, R., Adam, E., *Ann. Quim.*, **71** (1975) 1008.
- Fair, J. R., Lambright, A. J., Anderson, J. W., *Ind. Eng. Chem. Proc. Des. Dev.* **1** (1962) 33
- Deckwer, W. D., *Chem. Eng. Sci.*, **35** (1980) 1341.
- Nosier, S. A., *Chem. Eng. Tech.*, **26** (2003) 1151.
- Lewis, D. A., Field, R. W., Xavier, A. M., Edwards, D., *Trans. Inst. Chem. Eng.* **60** (1982) 40.
- Postlethwaite, J., Holdner, O. N., *Can. J. Chem. Eng.* **54** (1976) 255.
- Pini, G. C., Deanna, P. L., *Electrochim. Acta.* **1977** 1423.
- Prager, S., *Physica*, **29** (1963) 129.